



A Simple and Scalable Process for the Differentiation of Retinal Pigment Epithelium From Human Pluripotent Stem Cells

JULIEN MARUOTTI,^a KARL WAHLIN,^a DAVID GORRELL,^a IMRAN BHUTTO,^a GERARD LUTTY,^a
DONALD J. ZACK^{a,b,c,d,e}

Key Words. Retinal pigment epithelium • Pluripotent stem cells • Serum-free • Defined

ABSTRACT

Age-related macular degeneration (AMD), the leading cause of irreversible vision loss and blindness among the elderly in industrialized countries, is associated with the dysfunction and death of the retinal pigment epithelial (RPE) cells. As a result, there has been significant interest in developing RPE culture systems both to study AMD disease mechanisms and to provide substrate for possible cell-based therapies. Because of their indefinite self-renewal, human pluripotent stem cells (hPSCs) have the potential to provide an unlimited supply of RPE-like cells. However, most protocols developed to date for deriving RPE cells from hPSCs involve time- and labor-consuming manual steps, which hinder their use in biomedical applications requiring large amounts of differentiated cells. Here, we describe a simple and scalable protocol for the generation of RPE cells from hPSCs that is less labor-intensive. After amplification by clonal propagation using a myosin inhibitor, differentiation was induced in monolayers of hPSCs, and the resulting RPE cells were purified by two rounds of whole-dish single-cell passage. This approach yields highly pure populations of functional hPSC-derived RPE cells that display many characteristics of native RPE cells, including proper pigmentation and morphology, cell type-specific marker expression, polarized membrane and vascular endothelial growth factor secretion, and phagocytic activity. This work represents a step toward mass production of RPE cells from hPSCs. STEM CELLS TRANSLATIONAL MEDICINE 2013;2:000–000

INTRODUCTION

Age-related macular degeneration (AMD) is the leading cause of irreversible vision loss and blindness among the elderly in industrialized countries, affecting 30–50 million people worldwide [1]. An early event associated with AMD is damage to retinal pigment epithelium (RPE) cells [2]. The RPE abuts the photoreceptor cell layer and has many roles in visual function, including absorption of stray light, formation of the blood-retina barrier, transport of nutrients, secretion of growth factors, isomerization of retinol, and daily clearance of shed photoreceptor outer segments [3]. RPE dysfunction and cell death is associated with both the neovascular (“wet”) and atrophic (“dry”) forms of AMD [4]. Although effective anti-vascular endothelial growth factor (VEGF)-based treatments have been developed for the neovascular form of AMD, effective treatment options for the more common atrophic form of the disease are lacking [5, 6]. One approach being explored for the treatment of atrophic AMD is the transplantation of autologous RPE [7]. However, although a potentially promising approach, harvesting autologous RPE in-

volves complex surgery with possible sight-threatening complications [8, 9]. In addition, RPE harvested from an AMD patient, even if peripheral RPE is used as the source, runs the risk of being already impaired, because of the environmental and/or genetic factors that initially predisposed the patient to AMD.

An alternative approach to obtain human RPE cells is to generate them from human pluripotent stem cells (hPSCs), either from embryonic stem cells (hESCs) [10] or from induced pluripotent stem cells (hiPSCs) [11, 12]. Although no consensus has yet emerged regarding the equivalence of hiPSCs to hESCs [13–15], a striking feature of both cell types is their capacity for indefinite self-renewal while maintaining their potential to differentiate into all cell types of the human body. A number of investigators have demonstrated that cultured hiPSCs to hESCs can be induced to differentiate into cells that are phenotypically very similar to endogenous RPE cells. More than 10 years ago, Kawasaki et al. [16] described epithelial pigmented cells arising from differentiation of monkey ESCs on the mouse stromal cell line PA6. These cells were later

^aWilmer Eye Institute, ^bDepartment of Neuroscience, ^cDepartment of Molecular Biology and Genetics, and ^dInstitute of Genetic Medicine, Johns Hopkins University School of Medicine, Baltimore, Maryland, USA; ^eInstitut de la Vision, Université Pierre et Marie Curie, Paris, France

Correspondence: Donald J. Zack, M.D., Ph.D., Johns Hopkins University School of Medicine, 400 North Broadway, Baltimore, Maryland 21231, USA. Telephone: 410-502-5230; Fax: 410-502-5382; E-Mail: dzack@jhmi.edu

Received August 27, 2012; accepted for publication January 29, 2013; first published online in SCTM EXPRESS April 12, 2013.

©AlphaMed Press
1066-5099/2013/\$20.00/0

<http://dx.doi.org/10.5966/sctm.2012-0106>

shown to express RPE markers, to phagocytose latex beads *in vitro* and rod outer segments *in vivo*, and to alleviate to some extent photoreceptor degeneration following transplantation into Royal College Surgeon rats [17]. In 2004, Klimanskaya et al. [18] generated RPE cells through spontaneous differentiation of hESCs, whereas later on, RPE monolayers were successfully differentiated from hiPSCs [19–23]. hiPSCs could thus provide an unlimited supply of RPE-like cells for transplantation *in vivo* [24], as well as for research applications such as disease modeling and drug studies [25]. (For the sake of language simplicity, we will from this point forward refer to RPE-like cells derived from hiPSCs as “hiPSC-RPE cells.”) In several animal models, hiPSC-RPE cells have been shown to maintain their function after subretinal transplantation and to be able to attenuate retinal degeneration with partial preservation of visual function [17, 23, 26–29]. In addition, a human clinical trial based on hiPSC-RPE cell transplantation is currently under way [30].

Despite the success obtained with the generation of human RPE cells from hiPSCs, published protocols to date all rely on hiPSC amplification by clump passage and, following differentiation, on mechanical dissection of pigmented colonies for RPE purification [31, 32]. Both procedures, although powerful, are potentially problematic since they require time- and labor-consuming manual steps, which present challenge for scale-up and thereby constitute bottlenecks for large-scale production of high-quality and consistent hiPSC-RPE cells. In this study, we describe an RPE differentiation protocol that is less work-intensive than other methods described previously. In this new protocol, hiPSCs are amplified by clonal propagation using the myosin inhibitor blebbistatin [33, 34]. Subsequently, pigmented colonies are generated by spontaneous monolayer differentiation, and RPE cells are then enriched by two rounds of whole-dish single-cell passage. The procedure yields a highly purified cell population that displays many of the morphological, gene expression, and functional characteristics of native RPE cells. Completely defined conditions can be achieved through this protocol by the use of vitronectin peptide-acrylate surface (VN-PAS) [35] instead of Matrigel (BD Biosciences, San Diego, CA, <http://www.bdbiosciences.com>).

MATERIALS AND METHODS

Human Pluripotent Stem Cell Culture

Adapting a previously described method [33], the hESC line H7 (kind gift from Dr. Hai Quan Mao, Johns Hopkins University) and the hiPSC line IMR90-4 (WiCell Research Institute, Madison, WI, <http://www.wicell.org>) were maintained by clonal propagation either on growth factor-reduced Matrigel or on VN-PAS Synthemax (Corning Enterprises, Corning, NY, <http://www.corning.com>), in mTeSR1 medium (StemCell Technologies, Vancouver, BC, Canada, <http://www.stemcell.com>), in a 10% CO₂/5% O₂ incubator. For passaging, hiPSC colonies were first incubated with 5 μM blebbistatin (Sigma-Aldrich, St. Louis, MO, <http://www.sigmaaldrich.com>) in mTeSR1 and then collected after 5–10 minutes of treatment with Accutase (Sigma-Aldrich). Cell clumps were gently dissociated into a single-cell suspension and pelleted by centrifugation. Thereafter, hiPSCs were resuspended in mTeSR1 with blebbistatin and plated at approximately 1,000–1,500 cells per cm². Two days after passage, the medium was replaced with mTeSR1 (without blebbistatin) and then changed daily.

Differentiation and Culture of RPE From hiPSCs

Pluripotent stem cells were plated at 20,000 cells per cm² and maintained in TeSR1. Five days after passage, the cells formed a monolayer and were transferred to a 5% CO₂/20% O₂ incubator. Three days later, the culture medium was replaced with differentiation medium (DM) consisting of Dulbecco's Modified Eagle's Medium: Nutrient Mixture F-12 (DMEM/F12) (catalog no. 11330; Invitrogen, Carlsbad, CA, <http://www.invitrogen.com>), 15% knockout serum (Invitrogen), 2 mM glutamine (Invitrogen), 1× nonessential amino acids (Invitrogen), 0.1 mM β-mercaptoethanol (Sigma-Aldrich), and 1× antibiotic-antimycotic (Invitrogen). Approximately 25–30 days later, pigmented foci became clearly visible and were grown for an additional 25 days. At that point, the whole monolayer of differentiating cells was passaged a first time (P1) by incubation for 4 hours in DM supplemented with 0.25% (wt/vol) collagenase IV (Gibco, Grand Island, NY, <http://www.invitrogen.com>). The loosened cell monolayer was thereafter broken into small clumps by vigorous pipetting. These clumps were collected by centrifugation, resuspended in Accumax (Sigma-Aldrich), and incubated for 20–30 minutes at 37°C. After vigorous pipetting, most clumps were dispersed into single cells, and the solution was filtered through a 40-μm nylon mesh (BD Falcon, San Jose, CA, <http://www.bdbiosciences.com>). Differentiated cells were plated at 100,000 cells per cm² on Matrigel-coated or VN-PAS plates and allowed to grow for 15–20 days in RPE medium [36] consisting of 70% DMEM (Invitrogen), 30% Ham's F-12 Nutrient Mix (catalog no. 11765; Invitrogen), 1× B27 (Invitrogen), and 1× antibiotic-antimycotic (Invitrogen). For routine passage after P1, hiPSC-RPE cells were collected by using Accumax, pelleted by centrifugation, and replated at 100,000 cells per cm².

In control experiments, hiPSCs were cultured in mTeSR1 according to the manufacturer's instructions (clump-passage method). After differentiation in DM for 50 days, the pigmented foci were isolated by manual picking as previously [37], resuspended in Accumax (Sigma-Aldrich), and incubated for 20–30 minutes in a 37°C water bath. Dissociated clumps were then directly seeded onto Matrigel-coated plates and further passaged as described above. Characterization of hiPSC-RPE cells isolated through serial passage or by manual picking was performed at P2, after 50 days culture in RPE medium.

Human Fetal RPE Culture

Fetal RPE (fRPE) cells were obtained from ScienCell, plated at 50,000 cells per cm² on Matrigel, and cultured for 2 months in Epithelial Cell Medium (ScienCell, Carlsbad, CA, www.sciencellonline.com) before RNA was harvested.

Immunostaining

After fixation, the cells were blocked and permeabilized for 30 minutes in 5% goat serum, 0.25% Triton X-100 in PBS and then incubated overnight at 4°C with one of the following primary antibodies: rabbit anti-OCT4 1/500 (Abcam, Cambridge, U.K., <http://www.abcam.com>), rabbit anti-Nanog 1/1,000 (Millipore), rabbit anti-SOX2 1/1,000 (Millipore, Billerica, MA, <http://www.millipore.com>), mouse anti-SSEA4 1/100 (Millipore), mouse anti-MITF (C5) 1/100 (Thermo Fisher Scientific, Rockville, MD, <http://www.thermofisher.com>), mouse anti-ZO-1 1/500 (Invitrogen), mouse anti-BEST1 1/150 (Novus Biologicals, Littleton, CO, www.novusbio.com), mouse anti-RPE65 1/100 (Abcam), mouse anti-RLBP1 1/100 (Abcam), or rabbit anti-OTX2 1/500 (Millipore). The cells were then incubated for 1

hour with the corresponding secondary antibody conjugated to Alexa 488 or Alexa 647 (Invitrogen) and counterstained with Hoechst 33342 (Invitrogen).

Mouse eye cups were fixed in 2% paraformaldehyde in 0.1 M phosphate buffer with 5% sucrose. They were then cryoprotected in 20% sucrose in 0.1 M phosphate buffer and rapidly frozen in O.C.T. compound (Tissue-Tek; Sakura Finetek, Torrance, CA, <http://www.sakura.com>). Eight-micrometer sections were stained with 1/250 mouse anti-rhodopsin (Lab Vision, Fremont, CA, <http://www.labvision.com>) conjugated to Dylight 550 according to the manufacturer's instructions (Dylight 550 microscale antibody labeling kit; Pierce, Rockford, IL, <http://www.piercenet.com>) in 2% goat serum, 0.1% Triton X-100 in PBS. This was followed by incubation with Alexa Fluor 647 phalloidin (Invitrogen) and counterstaining with 4',6-diamidino-2-phenylindole.

Western Blot Analysis

hPSC-RPE proteins were extracted from cell lysates stored in RLT buffer (Qiagen, Hilden, Germany, <http://www.qiagen.com>) by acetone precipitation as previously [38] and resuspended in 1:1 vol/vol radioimmunoprecipitation (Sigma-Aldrich)-Laemmli buffer (Bio-Rad, Hercules, CA, <http://www.bio-rad.com>) with EDTA-free protease inhibitor cocktail (cComplete mini; Roche Applied Science, Indianapolis, IN, <https://www.roche-applied-science.com>). The protein concentrations were quantified using the EZQ protein quantification kit (Invitrogen). Approximately 10 μg per lane was resolved on a NuPAGE bis-tris gels (Invitrogen), and proteins were transferred to polyvinylidene difluoride membranes using the iBlot gel transfer system (Invitrogen). After a brief blocking step in SuperBlock Blocking Buffer (Thermo Scientific, Rockford, IL, <http://www.thermoscientific.com>) or 5% nonfat milk in Tris-buffered saline containing 0.1% Tween 20 (TBST), the membranes were incubated overnight with the following primary antibodies: rabbit anti-GAPDH 1/1,000 (Sigma-Aldrich), mouse anti-RLBP1 1/1,000 (Abcam), or mouse anti-BEST1 1/1,000 (Novus Biologicals). After several washes in TBST, the membranes were incubated in a 1/10,000 dilution of horseradish peroxidase (HRP)-conjugated anti-rabbit antibody (Santa Cruz Biotechnology Inc., Santa Cruz, CA, <http://www.scbt.com>) or 1:2,000 HRP-conjugated anti-mouse secondary antibodies (Cell Signaling Technology, Beverly, MA, <http://www.cellsignal.com>). After five washes in TBST, the membranes were incubated for 5 minutes in the SuperSignal West Femto Chemiluminescence Substrate (Pierce) and exposed to x-ray film (Kodak, Rochester, NY, <http://www.kodak.com>).

Flow Cytometry

For TRA-1-60, a cell surface marker, immunostaining was performed as previously [39], with a primary antibody concentration of 1 μg per 1 million cells. For intracellular and nuclear markers, immunostaining was performed using the IntraPrep permeabilization kit (Beckman Coulter, Fullerton, CA, <http://www.beckmancoulter.com>) according to the manufacturer's instructions. Primary antibody concentration was 1 μg per 1 million cells for mouse anti-RPE65 (Abcam) and mouse anti-MITF (C5) (Thermo Fisher Scientific) and 0.035 μg per 1 million cells for rabbit anti-OCT4 (Abcam). Secondary antibodies were either goat anti-mouse conjugated to Alexa 488 (Invitrogen) or goat anti-rabbit conjugated to Alexa 647 (Invitrogen). A nonspecific, species-appropriate isotype control was included in all flow cy-

tometry experiments, and stained cells were analyzed using an Accuri C6 flow cytometer (BD Biosciences, San Diego, CA, <http://www.bdbiosciences.com>). For each marker, analyses were performed on three biological repeats.

Phagocytosis Assay

The cells were incubated for 16 hours either at 4°C or 37°C in ambient air with 0.1 mg per cm^2 of pH-Rhodo-labeled bioparticles (Invitrogen) resuspended in CO_2 -independent medium (Invitrogen) supplemented with 4 mM glutamine (Invitrogen) and 1 \times antibiotic-antimycotic (Invitrogen). Afterwards, the cells either were fixed and immunostained or were dissociated and analyzed by flow cytometry.

VEGF Enzyme-Linked Immunosorbent Assay

RPE cells derived from hPSCs were grown on Transwell membrane (Corning) coated with Matrigel or VN-PAS Synthmax II SC (Corning). Cell culture supernatants from the hPSC-RPE cell apical and basal sides, that is, upper and lower compartments of the Transwell, respectively, were collected after 48 hours of cell culture and sent on dry ice to Antigen Targeting and Consulting Service (Worcester, MA, <http://www.atcs-incorporated.com>). VEGF-A measurements were done in duplicate.

Transplantation of Carboxyfluorescein Diacetate Succinimidyl Ester-Labeled hPSC-RPE Cells

hESC-RPE cells were cultured for 20 days after plating, until they formed a lightly pigmented monolayer suitable for transplantation [30]. The cells were then labeled with 25 μM carboxyfluorescein diacetate, succinimidyl ester (CFSE) (CellTrace CFSE cell proliferation kit; Invitrogen) for 15 minutes at 37°C. The next day, the hESC-RPE cells were resuspended in RPE medium.

NOD-scid mice (NOD.CB17-Prkdesid/J, 8–10 weeks old; Jackson Laboratory, Bar Harbor, ME, <http://www.jax.org>) were anesthetized by i.p. injection of a mixture of ketamine and xylazine. After making a hole at the pars plana with a 30-gauge sterile needle (BD Biosciences), a micropipette glass needle (tip internal diameter of 25–30 μm) mounted on a Pico-Injector holder (PLI-100; Harvard Apparatus, Holliston, MA, www.harvardapparatus.com) was inserted through the hole into the vitreous, stopping at the surface of the retina. One microliter of the hESC-RPE cell suspension ($5 \times 10^4/\mu\text{l}$) was delivered into the subretinal space of each eye. Fundus photographs of the retina were taken every other day with a Micron III imager (Phoenix Research Lab, Inc., Pleasanton, CA, www.phoenixreslabs.com).

All of the surgical and animal care procedures were performed in compliance with the guidelines for care and use of laboratory animals of Johns Hopkins University and the Association for Research in Vision and Ophthalmology statement for the use of animals in ophthalmic and visual research.

Reverse Transcription-Polymerase Chain Reaction and Quantitative Real-Time Polymerase Chain Reaction

Total RNAs were extracted (RNeasy Mini Kit) and treated with RNase-free DNase I (both from Qiagen). Extracted RNAs were reverse-transcribed (High Capacity cDNA kit; Applied Biosystems, Foster City, CA, <http://www.appliedbiosystems.com>), reverse transcription-polymerase chain reactions (RT-PCRs) were performed with PCR SuperMix (Invitrogen), and quantitative

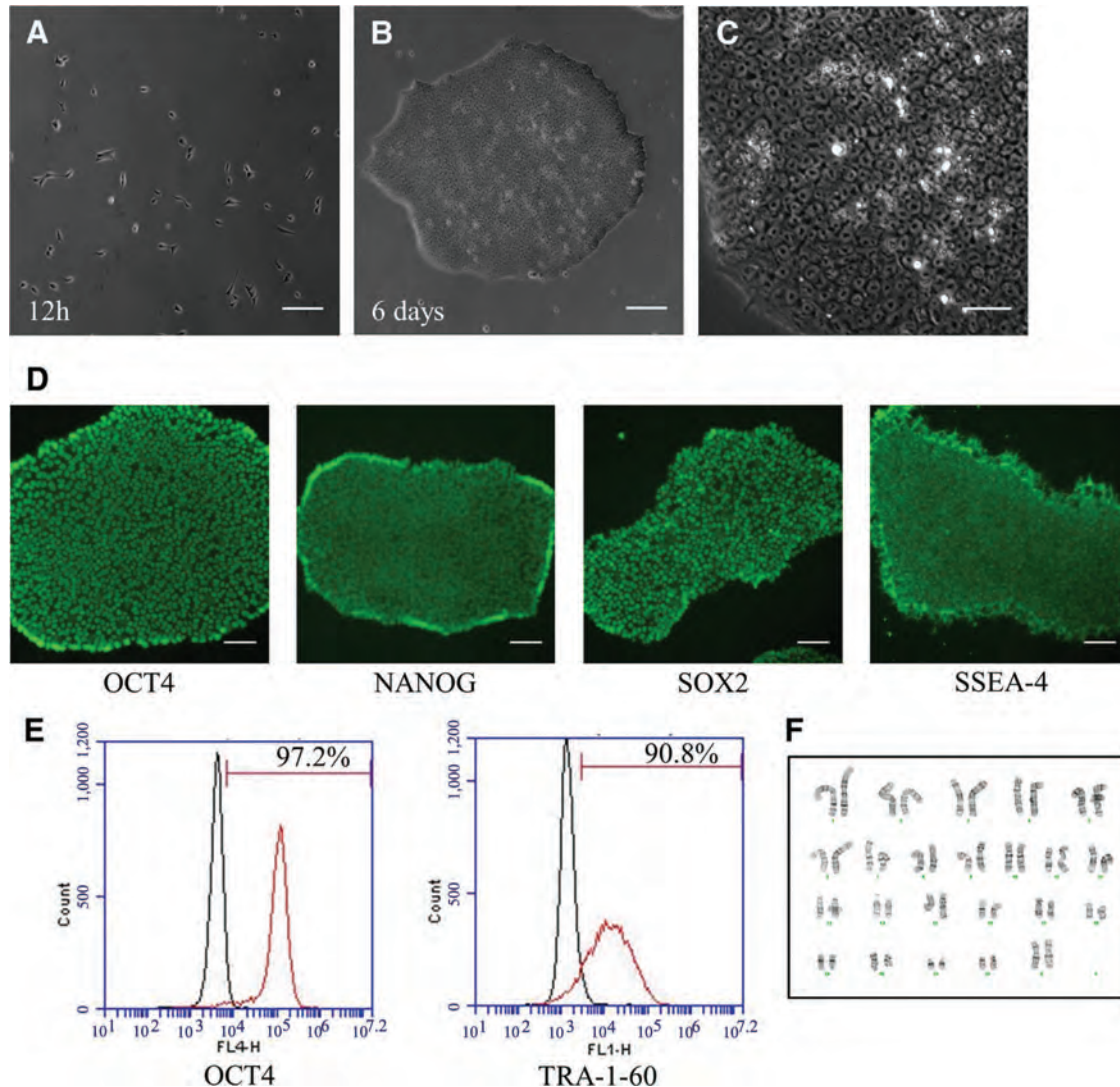


Figure 1. Long-term culture of human pluripotent stem cells (hPSCs) by clonal propagation. After plating of single cells, characteristic-looking hPSC colonies formed over the next several days. **(A, B):** Phase contrast photomicrographs showing the morphology of hPSC colonies after 12 hours and 6 days of culture, respectively. Scale bars = 100 μm . **(C):** Enlargement of **(B)** displaying hPSCs with typical pluripotent morphology (large nuclei and clear cytoplasm). Scale bar = 30 μm . **(D):** Expression of key pluripotency markers by immunostaining, after 6 days of culture. Scale bars = 50 μm . **(E):** Flow cytometric analysis of the expression of OCT4 and TRA-1-60 in hPSCs cultured for 6 days. The profile of cells stained with the indicated antibody is shown in red, and the isotype control is displayed in black. **(F):** G-banded karyotype analysis of an hPSC line.

real-time PCRs (qPCRs) were performed with EvaGreen qPCR Mastermix (Abm, Richmond, BC, Canada, <http://www.abmgood.com>). Quantitative PCR samples were run in triplicate, and expression levels were normalized using the geometric mean of three reference genes: FBXL12, SRP72, and CREBBP [40]. Gene-specific primers (supplemental online Tables 1, 2) were obtained from published sequences or designed using Beacon Designer (PREMIER Biosoft, Palo Alto, CA, www.premierbiosoft.com). RNA from M1, a primary culture of RPE derived from an adult donor eye, was a kind gift from Dr. Noriko Esumi (Johns Hopkins University).

Statistical Analysis

Analysis of variance (Tukey test) analysis was done with Prism 6.01 (GraphPad Software, Inc., San Diego, CA, <http://www.graphpad.com>).

RESULTS

hPSCs Maintain Pluripotency and Normal Karyotype After Long-Term Culture by Clonal Propagation

Based on a previous report that hPSCs can be successfully propagated through the use of blebbistatin [33], we first checked whether the hiPSC and hESC lines that we were using could also be cultured long term following this approach. When cultured by clonal propagation, hPSCs grew from single cells (Fig. 1A) to large colonies ready for passage within approximately a week (Fig. 1A, 1B; supplemental online Fig. 1A). These colonies displayed morphological features typical of pluripotent cells, such as a smooth surface and tightly packed cells with large nuclei (Fig. 1C; supplemental online Fig. 1B). (Data obtained with Matrigel are reported in the main figures of the article, whereas data obtained with VN-PAS are shown in the supplemental figures except when otherwise noted.)

After more than 20 passages (>3 months) by clonal propagation, expression of key markers of pluripotency such as POU class 5 homeobox 1 (POU5F1, also known as OCT4), Nanog homeobox (NANOG), sex-determining region Y (SRY) box 2 (SOX2), and the cell surface antigen SSEA-4 were all observed in a majority of hPSC colonies, as assessed by immunostaining (Fig. 1D; supplemental online Fig. 1C). Confirming these results, flow cytometry analysis indicated that >97% of cells in culture stained positive for OCT4, whereas >91% were positive for the cell surface antigen TRA-1-60 (Fig. 1E; supplemental online Fig. 1D; supplemental online Table 3). Spontaneous differentiation was therefore minimal and comprised between 3% and 9% of the total cell population, according to the pluripotency marker assessed. Finally, chromosome integrity was evaluated by G-banding karyotype: for both hPSC lines, the majority of the 20 metaphase spreads analyzed were found to have a normal 46, XX karyotype (Fig. 1F; supplemental online Fig. 1E). Taken together, these data confirm earlier results and show that hPSCs can be cultured for extended periods of time on Matrigel or VN-PAS by clonal propagation while maintaining a high level of pluripotent marker expression and a stable karyotype.

Differentiation of hPSC Monolayers Is Associated With Progressive Expression of RPE Markers

In order to induce differentiation of hPSCs, cells were plated at high density (20,000 cells per cm²) in TeSR1 and cultured for 8 days, during which time the cells developed into a monolayer (Fig. 2A). At that point, the pluripotency maintaining medium was exchanged for differentiation medium (DM; see Materials and Methods). Following this protocol, spontaneously differentiating monolayers of hPSCs reproducibly generated RPE cells after several weeks [22, 23, 26]. For the first weeks, the differentiating monolayer remained colorless, and pigmented colonies typically started to be visible 25–30 days after the switch to DM (d1) (supplemental online Fig. 2). In order to understand the kinetics of RPE differentiation following d1, we monitored the expression of several markers by qPCR on a weekly basis (Fig. 2B). Expression of the pluripotency marker *OCT4* was rapidly downregulated and became undetectable by week 3. Expression of the eye field transcription factor paired box 6 (*PAX6*) was clearly evident by week 1, with some increased expression over the next few weeks. Microphthalmia-associated transcription factor (*MITF*), a transcription factor (TF) required for RPE differentiation [41], showed a similar pattern of expression. In contrast, orthodenticle homeobox 2 (*OTX2*), another TF involved in RPE differentiation [41], was already highly expressed in hPSCs as previously [42], became downregulated from week 1 to week 2, and then showed little additional change. We also checked mature RPE markers and found that bestrophin 1 (*BEST1*), retinaldehyde-binding protein 1 (*RLBP1*), and retinal pigment epithelium-specific protein of 65 kDa (*RPE65*) all showed early detectable levels of expression that generally increased with time in DM. More specifically, *BEST1*, which encodes a chloride channel-related protein, was upregulated approximately three- to eightfold from week 1 to week 3, and *RLBP1* and *RPE65*, which encode proteins responsible for the visual cycle, were both upregulated approximately fivefold during the same time interval. Tyrosinase (*TYR*), which encodes the enzyme responsible for the conversion of tyrosine to the pigment melanin, was undetectable during the first 2 weeks of differentiation. It is noteworthy that its expression increased markedly after the third week of

differentiation, which correlated with the appearance of the first pigmented colonies in our cultures. Our results demonstrated that during the first 5 weeks of RPE differentiation, hPSCs gradually upregulate key RPE markers while downregulating the expression of pluripotency maintaining TFs.

Approximately 50 days after switching to DM, numerous large clusters of pigmented cells were readily observed in our cultures (Fig. 2C; supplemental online Fig. 2C). In order to assess the extent of differentiation toward putative RPE, we sought to analyze the cell monolayers by flow cytometry for expression of RPE65. Because monolayers of differentiating cells are difficult to dissociate into single-cell suspensions required for flow cytometry procedures, we first incubated them for an extended period of time in DM supplemented with collagenase IV. Upon prolonged incubation with collagenase, the monolayers detached and formed many small clumps. These clumps were then easily dissociated to single cells by treatment with Accumax. Following this approach, we were able to reproducibly obtain monocellular solutions of differentiating cells suitable for flow cytometry analysis. We found that the fraction of RPE65+ cells did not significantly differ between hiPSCs and hESCs, being $16.1 \pm 0.2\%$ and $16.6 \pm 2.5\%$, respectively (Fig. 2D, 2E).

Enrichment of Putative RPE From hPSCs Leads to Monolayers of Pigmented Cells With Polygonal Morphology

Since it was possible to generate single-cell suspensions of differentiating hPSCs consisting of approximately 16% with RPE characteristics, we decided to further culture these cells. After 50 days in DM, whole dishes of differentiating hPSCs were passaged a first time (P1) by successive treatment with collagenase IV and Accumax (Fig. 2A). The cells were then plated at high density (100,000 cells per cm²) and cultured in RPE medium (see Material and Methods). Two weeks after P1, we observed that the dishes contained many large colonies consisting of lightly pigmented cells with characteristic cobblestone morphology (Fig. 3A). These colonies were intermingled with nonpigmented cells with a fibroblast-like morphology. In order to further enrich the culture for putative RPE cells, we thereafter passaged the whole dish a second time (P2) and cultured the cells as before. One month after P2, the cells had grown into a monolayer of lightly pigmented cells with cobblestone morphology (not shown). Surprisingly, there were no longer detectable nonpigmented fibroblast-like cells like those observed at P1. For characterization, the putative RPE monolayers were then allowed to mature for an additional 20 days (Fig. 2A). At that point, 50 days after P2, RPE cells were strongly pigmented and had a polygonal morphology (Fig. 3B, 3C; supplemental online Fig. 3A, 3B). The monolayer had formed many domes (not shown), suggesting that the cells were functional and engaged in active fluid transport, as is known to occur in mature tight junction-bearing RPE cells [3]. As an alternative way to maintain the hPSC-RPE cells, we were able to serially passage them every 15–20 days after P2.

hPSC-RPE Cells Form Polarized Monolayers and Express Key RPE Genes and Proteins

We used immunohistochemistry to characterize the expression of key RPE proteins by the enriched hPSC-RPE cell monolayers.

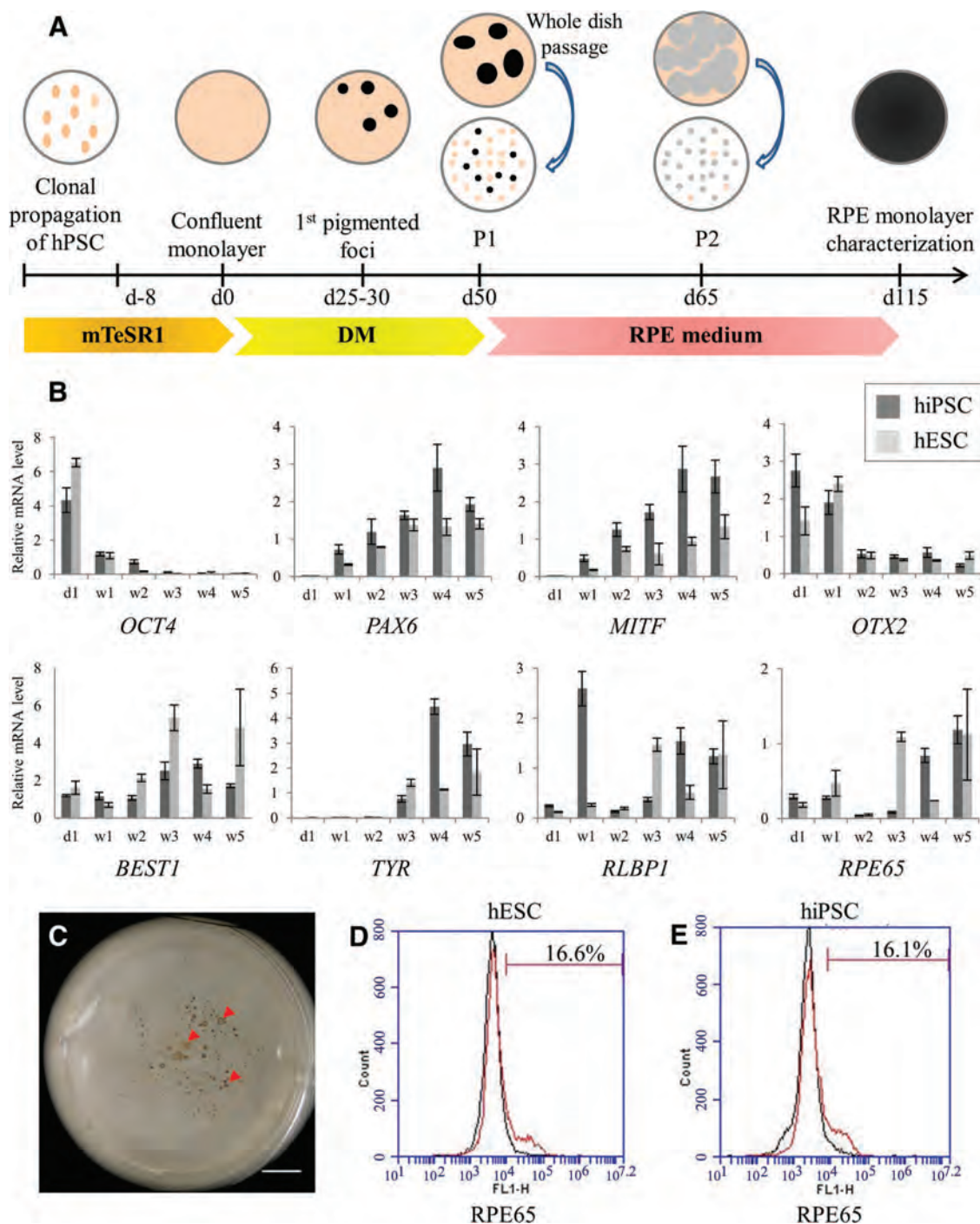


Figure 2. Differentiation of hPSCs into RPE. **(A):** Schematic view of the differentiation process. **(B):** Kinetics of marker expression of differentiating hESCs and hiPSCs as measured by quantitative real-time polymerase chain reaction. d1 denotes the time at which the cells were transferred to DM. Error bars represent standard deviation of biological replicates. **(C):** Morphology of hPSCs after 50 days in DM, with arrowheads indicating representative pigmented colonies. Scale bar = 5 mm. **(D, E):** Flow cytometric analysis of the expression of RPE65 by differentiating hPSCs after 50 days in DM. The profile of cells stained with the anti-RPE65 antibody is shown in red, and the isotype control is displayed in black. Only a minority of cells were RPE65-positive, which is in accordance with the limited number of pigmented colonies obtained in **(C)**. Abbreviations: d, day of the experiment; DM, differentiation medium; hESC, human embryonic stem cell; hiPSC, human induced pluripotent stem cell; hPSC, human pluripotent stem cell; P1, first passage; P2, second passage; RPE, retinal pigment epithelium; w, week.

We detected strong expression of MITF and OTX2 (Fig. 3D; supplemental online Fig. 3C). In addition, we observed strong membrane staining of BEST1 and the tight junction protein ZO-1 (Fig. 3D; supplemental online Fig. 3C), which showed basolateral and

apical localization, respectively (Fig. 3G, 3H; supplemental online Fig. 3D, 3E). This polarized expression of ZO-1 and BEST1 is in accordance with patterns described previously in both hPSC-RPE cells [22, 23, 26] and fetal RPE cells [36, 43] cultured in vitro, as

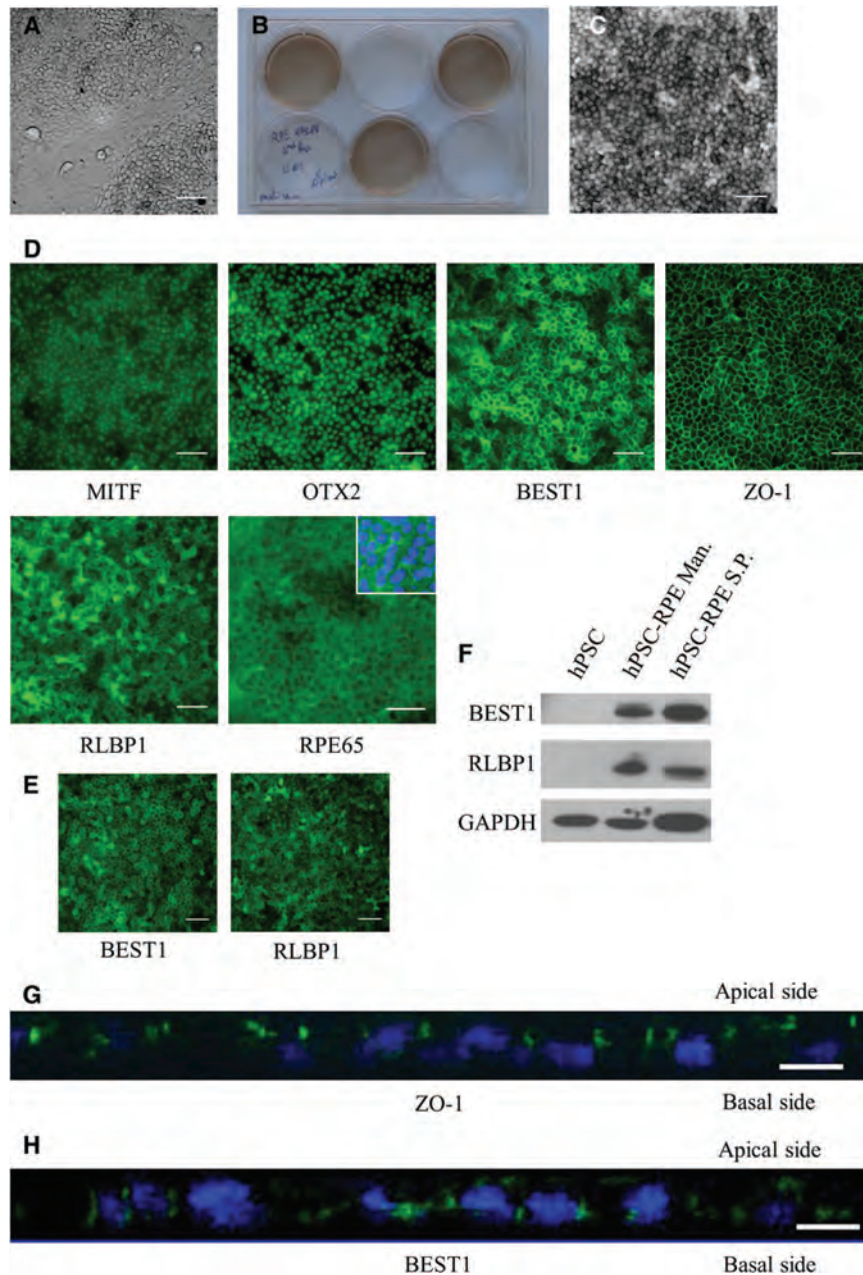


Figure 3. Morphology of hPSC-RPE cells and expression of RPE marker proteins in pigmented monolayers. **(A):** Bright-field photomicrograph of hPSC-RPE colonies intermingled with fibroblast-like cells after passage 1. Scale bar = 30 μm . **(B):** A six-well plate with hPSC-RPE cells after 50 days of maturation in RPE medium. **(C):** Bright-field photomicrograph of hPSC-RPE cells shown in **(B)**. Scale bar = 30 μm . **(D):** Expression of key RPE markers by immunostaining. Scale bars = 30 μm . **(E):** Expression of BEST1 and RLBP1 in hPSC-RPE cells obtained by manual picking. Scale bars = 30 μm . **(F):** Western blot analysis of BEST1 and RLBP1 expression. A protein standard was used on each Western blot to determine the correct molecular weight of proteins. **(G, H):** z-stack confocal micrographs showing typical polarized expression of RPE proteins, with ZO-1 (green) demonstrating apical localization **(G)** and BEST1 (green) demonstrating basolateral localization **(H)**. The nuclei were counterstained with Hoechst (blue). Scale bars = 10 μm . Abbreviations: GAPDH, glyceraldehyde-3-phosphate dehydrogenase; hPSC, human pluripotent stem cell; Man., manual picking; RPE, retinal pigment epithelium; S.P., serial passage.

well as in adult RPE in vivo [44, 45]. Finally, the visual cycle proteins RLBP1 and RPE65 showed clear expression in most hPSC-RPE cells (Fig. 3D; supplemental online Fig. 3C). Interestingly, BEST1 and RLBP1 had a more heterogeneous staining pattern, similar to what was observed in hPSC-RPE cells obtained by manual picking (Fig. 3E). We also confirmed by Western blot that these mature RPE markers were expressed at comparable levels in hPSCs obtained by serial passage and manual picking (Fig. 3F). Taken together, these results demonstrate that hPSC-RPE cells

form polarized monolayers that express many important RPE proteins.

Next, we further analyzed hPSC-RPE gene expression by RT-PCR. In addition to *MITF* and *OTX2*, detected previously by immunostaining, we also examined the expression of genes playing a role in RPE function (Fig. 4A). We observed strong expression of transcripts for *TYR* and premelanosome protein (*PMEL*), both involved in melanogenesis. Related to retinoid recycling, *RLBP1*, *CRALBP*, and lecithin retinol acyltransferase (*LRAT*) transcripts

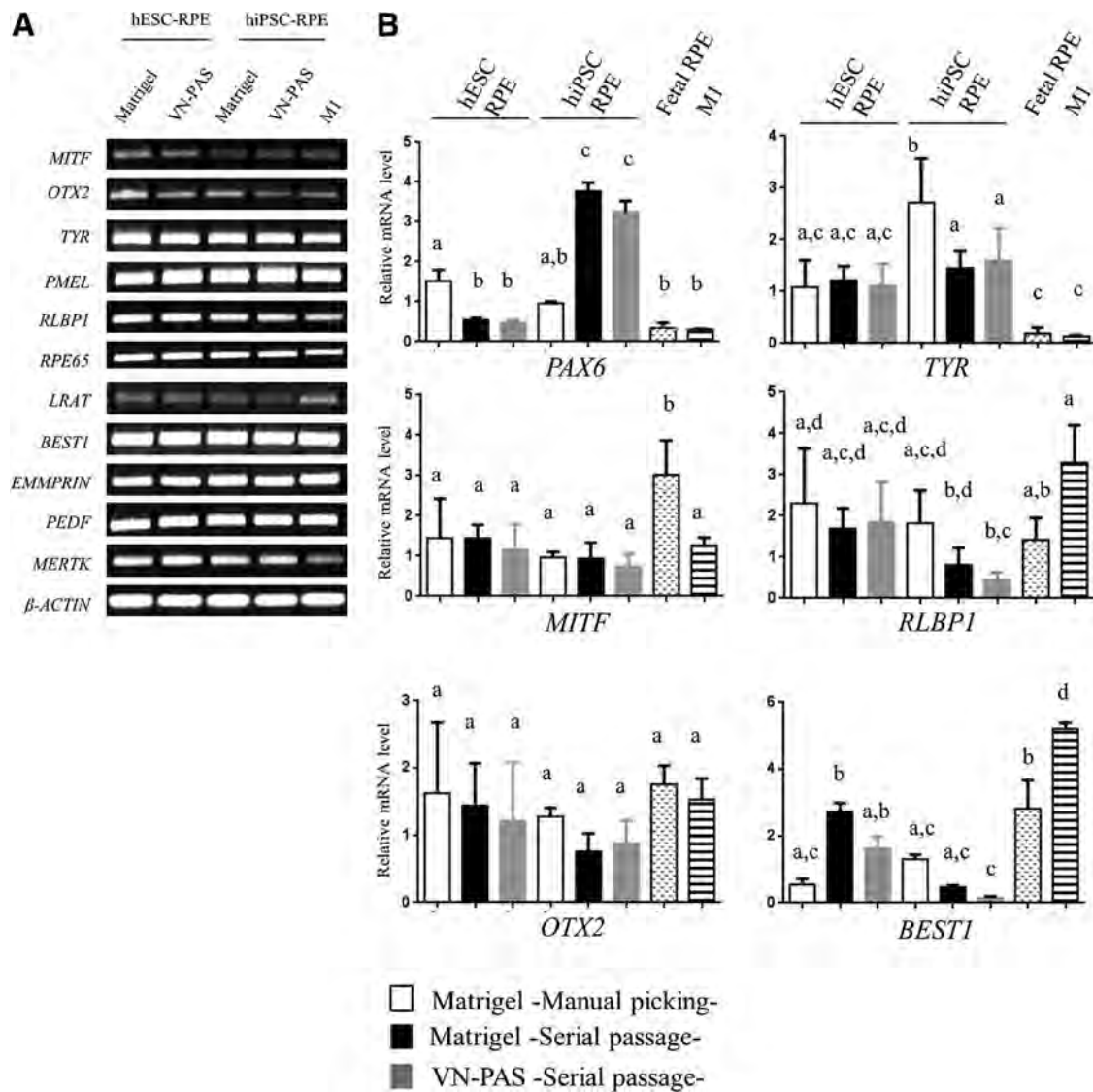


Figure 4. Expression of RPE gene transcripts in hPSC-RPE cells. **(A):** Reverse transcription-polymerase chain reaction (PCR) analysis of RPE markers expressed by hPSC-RPE cells cultured on Matrigel or VN-PAS. **(B):** Quantitative real-time PCR analysis of key RPE markers expressed by hPSC-RPE cells obtained after manual picking or serial passage. For each histogram, expression levels with different letters were significantly different ($p < .05$). Error bars represent standard deviation. Note: for BEST1, comparison between manually picked hiPSC-RPE cells on Matrigel and serial passage hiPSC-RPE cells on Synthemax gave a p value of .075 in the analysis of variance, whereas it was .008 after t test. Abbreviations: hESC, human embryonic stem cell; hiPSC, human induced pluripotent stem cell; hPSC, human pluripotent stem cell; RPE, retinal pigment epithelium; VN-PAS, vitronectin peptide-acrylate surface.

were detected. In addition to *BEST1*, transcripts for another membrane-associated protein, the extracellular matrix metalloproteinase inducer (*EMMPRIN*) [46], were expressed. Transcripts for pigment epithelium-derived factor (*PEDF*), an antiangiogenic neurotrophin secreted apically by RPE cells [47], were detected at high levels in hPSC-RPE cells, as were transcripts for c-met proto-oncogene tyrosine kinase (*MERTK*), which is associated with phagocytosis [48]. Overall, hPSC-RPE cells cultured on Matrigel or VN-PAS express all the expected RPE markers that we tested for.

The extracellular matrix (ECM) has been shown to play an important role in RPE differentiation and hPSC-RPE gene expression [49]. We therefore sought to understand whether the two ECMs used in our study had an influence on RPE marker expression, as determined by qPCR. We did not detect any significant

difference ($p > .05$) in gene expression for hESC-RPE or hiPSC-RPE cells grown on VN-PAS compared with Matrigel (Fig. 4B). Next, we compared mRNA expression levels between hPSC-RPE cells obtained after manual picking and those obtained after serial passage (Fig. 4B). Interestingly, we found *PAX6* to be significantly upregulated, approximately 3.5-fold in hiPSC-RPE cells obtained by serial passage versus manual picking. On the other hand, *PAX6* in hESC-RPE cells obtained by serial passage was downregulated approximately threefold compared with hESC-RPE cells obtained by manual picking. Since *PAX6* expression is observed during RPE development *in vivo* but turned down as RPE matures [50], this result could suggest that for hiPSCs, serial passage may lead to RPE in a less mature state compared with manual picking, whereas the opposite may be true for hESCs. The other RPE markers analyzed showed minimal differences, with the

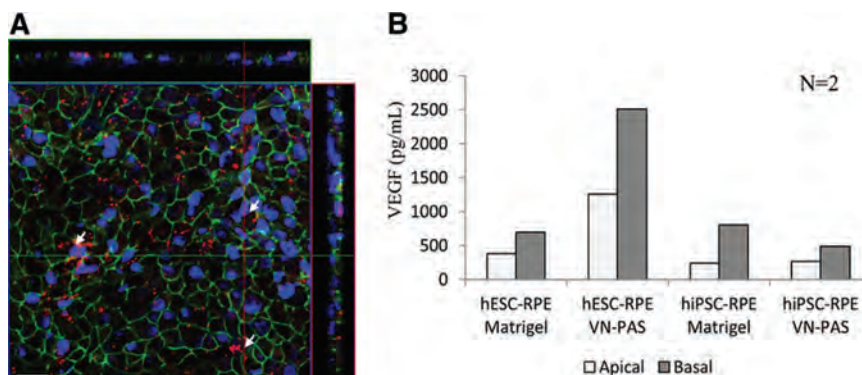


Figure 5. Functional analysis of human pluripotent stem cell (hPSC)-RPE cells. **(A):** Confocal micrograph showing phagocytosis of pH-Rhodo-labeled bioparticles (red) by hPSC-RPE cells (arrows). The apical sides of hPSC-RPE cells are stained with ZO-1 (green), whereas nuclei are counterstained with Hoechst (blue). Scale bar = 20 μm . **(B):** Polarized secretion of VEGF-A from the apical and basal sides of hPSC-RPE cells grown on Transwells. The bars represent the averages of duplicate experiments. Abbreviations: hESC, human embryonic stem cell; hiPSC, human induced pluripotent stem cell; RPE, retinal pigment epithelium; VEGF, vascular endothelial growth factor; VN-PAS, vitronectin peptide-acrylate surface.

only differences above twofold not being statistically significant. However, there was a trend toward lower expression of the mature marker *BEST1* in hiPSC-RPE cells obtained after serial passage (p values of .438 and .075 for manual vs. serial passage on Matrigel or vs. serial passage on VN-PAS, respectively), whereas the trend was toward higher expression levels for hESC-RPE cells isolated after serial passage (p values of $<10^{-4}$ and .11 for manual vs. serial passage on Matrigel or vs. serial passage on VN-PAS, respectively). Finally, we compared hPSC-RPE cells obtained after serial passage with cultured fRPE cells and M1, a primary line of adult RPE cells [51] (Fig. 4B). hPSC-RPE cells had overall lower mRNA levels for *BEST1*, whereas the opposite was true for *TYR*, a finding similar to results reported previously [22]. With the exception of *PAX6* in hiPSC-RPE cells and *MITF* in fRPE cells, gene expression levels were otherwise comparable between hPSC-RPE and native RPE cells for the other markers analyzed.

Together, these findings indicate that culturing hPSC-RPE cells on Matrigel versus VN-PAS does not significantly impact their gene expression profile, at least for the key RPE markers assessed. Similarly, RPE purification by serial passage did not significantly influence hPSC-RPE mRNA levels compared with manual picking, except for *PAX6*, where an opposite effect was observed in hESCs and hiPSCs. Finally, we did note differences in transcript abundance between hPSC-RPE and fRPE or M1, consistent with previous reports that hPSC-derived RPE cells are not exactly equivalent to native RPE at the transcriptional level [52].

hPSC-RPE Cells Form Functional Monolayers Capable of Phagocytosis and Polarized Secretion of VEGF

An essential function assumed by RPE cells in vivo is the phagocytosis of outer segments shed by photoreceptors [3]. In order to test whether hPSC-RPE cells were capable of such phagocytosis, they were first incubated in the presence of pH-Rhodo-labeled bioparticles, fixed, and stained for the tight junction protein ZO-1, which marks the apical side of RPE cells. It is only upon entering low pH phagosomes that pH-Rhodo-labeled bioparticles become fluorescent, thus providing a convenient system to observe particles specifically engulfed by cells. Apically localized pH-Rhodo-labeled bioparticles were extensively observed within hPSC-RPE layers (Fig. 5A; supplemental online Fig. 4), indicating that these cells were capable of phagocytosis.

RPE cells in vivo are also known to secrete growth factors, such as VEGF, in a polarized fashion [3]. Similarly, native RPE monolayers in vitro show preferential secretion of VEGF to the basal side [43]. We therefore grew hPSC-RPE cells on Transwells and collected culture medium from both the upper and lower reservoirs, as has been described previously [53]. We found that VEGF was preferentially secreted by the basal side of hPSC-RPE cells, with basal to apical ratios ranging from 1.8 to 3.3 (Fig. 4C). Intriguingly, VEGF secretion levels were higher for hESC-RPE cells cultured on VN-PAS, with concentrations as high as 2,500 and 1,255 pg/ml for the basal and apical sides, respectively. In contrast, VEGF levels for hESC-RPE cells maintained on Matrigel were comparable to those observed for hiPSC-RPE cells with both ECMs: they ranged from close to 500 pg/ml up to 700 pg/ml for the basal side and between 250 and 380 pg/ml for the apical side.

Taken together, these results demonstrate that hESC-RPE and hiPSC-RPE cells generated through our new protocol, whether grown on Matrigel or on VN-PAS, are functional, showing both phagocytic activity and polarized growth factor secretion.

hPSC-RPE Monolayers Obtained After Serial Passage Have the Same Degree of Cell Purity as hPSC-RPE Cells Obtained After Manual Isolation

Since our protocol to obtain hPSC-RPE monolayers did not feature any isolation step but was rather based on progressive enrichment by serial passage, it was important to assess the degree of cell purity. To this end, hPSC-RPE monolayers obtained through serial passage or by manual picking were immunostained for MITF or RPE65 and analyzed by flow cytometry (Fig. 6A). hPSC-RPE cells obtained by serial passage were found to be 96.9%–99.1% positive for MITF, values similar to that observed with hPSC-RPE cells obtained by manual picking (99.3%–99.5%) (supplemental online Table 4). For RPE65, 97.6%–98.5% of cells expressed this marker in the case of hPSC-RPE cells cultured on Matrigel after both serial passage and manual picking. Interestingly, although hESC-RPE cells maintained on VN-PAS were over 98% positive for RPE65 expression, hiPSC-RPE cells maintained on the same surface demonstrated RPE65 expression in only 68% of the cells (supplemental online Fig. 4B). Surprised by this result, we repeated the experiment with hiPSC-RPE cells from a different batch of differentiated cells and obtained a similar fraction of RPE65+ cells (data not shown). This could mean that, in the case of hiPSCs differentiated on VN-PAS, enrichment by serial

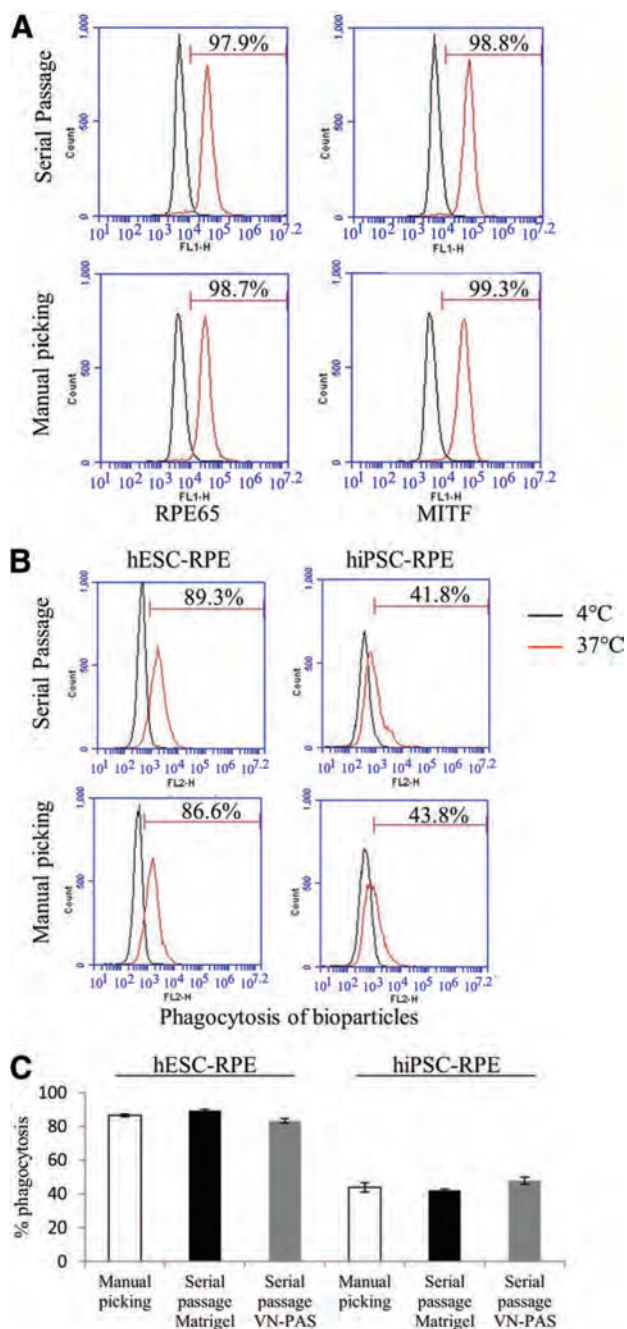


Figure 6. Flow cytometric analysis of human pluripotent stem cell (hPSC)-RPE cells. **(A):** Flow cytometric analysis of the expression of RPE65 and MITF in hPSC-RPE cells obtained after manual picking or serial passage and grown on Matrigel for 50 days after the second passage. The profile of cells stained with the anti-RPE65 or anti-MITF antibody is shown in red, and the isotype control is displayed in black. **(B):** Flow cytometric analysis of hPSC-RPE cell phagocytosis. The level of incorporation of pH-Rhodo-labeled bioparticles after incubations for 16 hours at 37°C is shown in red. As a negative control, since active phagocytosis is temperature-dependent, samples of hPSC-RPE cells were incubated at 4°C (black profile). **(C):** Comparison of pH-Rhodo-labeled bioparticle phagocytosis for hPSC-RPE cells obtained after manual picking or through serial passage. Abbreviations: hESC, human embryonic stem cell; hiPSC, human induced pluripotent stem cell; RPE, retinal pigment epithelium; VN-PAS, vitronectin peptide-acrylate surface.

passage is not complete, and a significant number of MITF+/RPE65– cells still contaminate the RPE monolayer. Visual observation under the microscope did not reveal any extended area of non-pigmented cells in hiPSC-RPE cells differentiated on VN-PAS, as would be expected from a contamination of almost 30% by non-RPE cells. Nevertheless, contamination could be due to melanocytes, which are MITF+ pigmented cells [54] expressing RPE65 protein at very low level compared with the RPE [55]. To test this possibility, PCR analysis for the melanocyte transcription factor *PAX3* was carried out with the hiPSC-RPE cells grown on VN-PAS. The assay failed to detect any *PAX3* expression (data not shown). Thus, the diminished ratio of RPE65+ cells does not seem to have been caused by melanocyte contamination; it more probably is a consequence of a lower level of RPE65 protein expression that is below the level detectable by our flow cytometry assay. Supporting this hypothesis, the median fluorescence intensity of RPE65 stained cells was approximately two times lower for hiPSC-RPE cells grown on VN-PAS versus Matrigel (supplemental online Fig. 4B).

To further characterize the functionality and consistency of the hPSC-RPE cells, we used a previously described phagocytosis assay [30]: pH-Rhodo-labeled bioparticles were seeded on hPSC-RPE monolayers, and the cells were incubated at 37°C and then analyzed by flow cytometry (Fig. 6B). Compared with controls incubated at 4°C, a temperature that inhibits phagocytosis, 89 and 83% of hESC-RPE cells cultured on Matrigel or VN-PAS, respectively, had phagocytosed pH-Rhodo-labeled bioparticles (Fig. 6C). This result was equivalent to that of hESC-RPE cells isolated by manual picking (87%) and close to that published in a previous study [30]. In contrast, the percentage of cells with phagocytosed particles was almost two times lower for hiPSC-RPE cells, ranging from 42% to 48%, regardless of the extracellular matrix used or the purification protocol followed. In summary, these data show that hPSC-RPE cells obtained after serial passage have a high degree of cell purity and that they are comparable to hPSC-RPE cells isolated by manual picking in terms of the fraction of functional RPE cells.

hPSC-RPE Cells Transplanted In Vivo Survive and Remain Functional

In order to test the ability of hPSC-RPE cells to survive in an in vivo setting, CFSE-labeled hESC-RPE cells were injected into the subretinal space of albino, NOD-scid mice. Fundus images taken 1 week later displayed the presence of numerous pigmented clusters in the injected area, suggesting that the hESC-RPE cells had survived the transplantation process (Fig. 7A). Retinal sections showed that hESC-RPE cells formed boluses in the subretinal space (Fig. 7B), as has been described previously at this time point [23]. Importantly, the presence of rhodopsin-positive fragments within the cellular contours of hESC-RPE cells (delineated by F-actin staining) indicates that these cells can phagocytose photoreceptor outer segments from the mouse retina (Fig. 7B, arrowheads).

DISCUSSION

We have described here, as a modification of a standard protocol for the isolation of RPE from spontaneously differentiating hPSC monolayers [18, 37], a method by which hPSCs are amplified by clonal propagation and in which RPE cells are enriched by serial passage instead of by mechanical picking. These modifications eliminate the need for the time- and labor-consuming manual steps usually required to culture hPSCs and to purify the RPE population and thereby provide a readily scalable approach to generate large

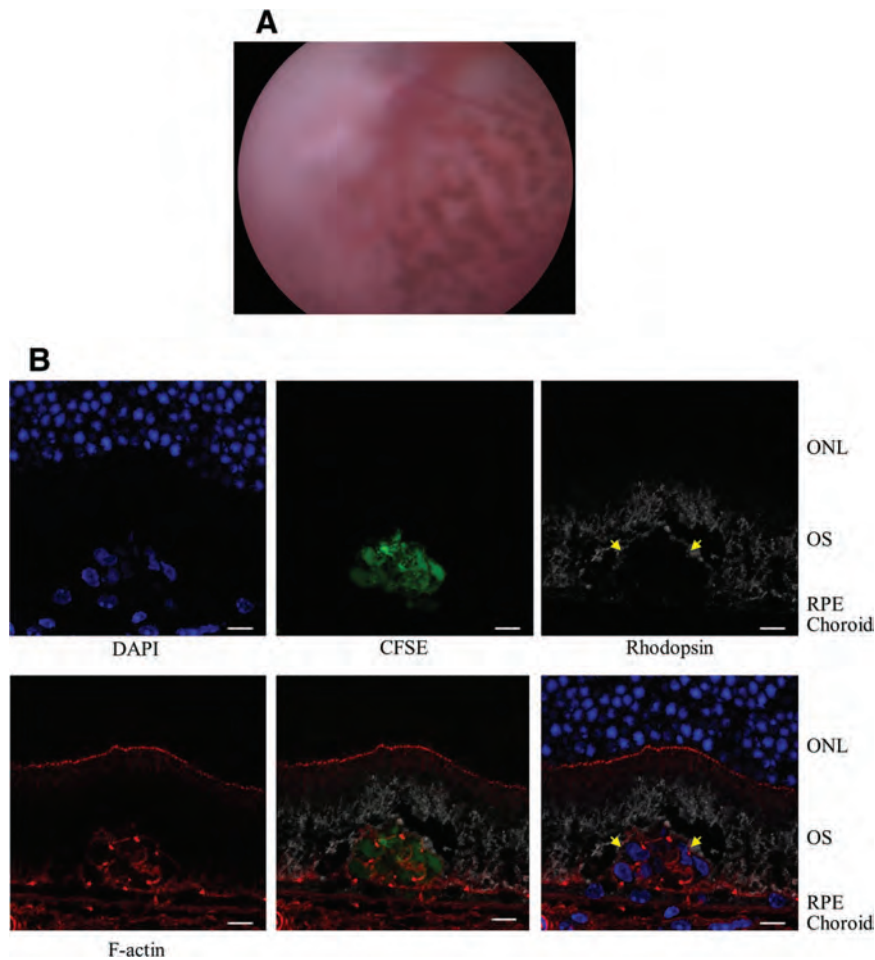


Figure 7. Transplantation of human pluripotent stem cell (hPSC)-RPE cells into the subretinal space of albinos NOD-scid mice. **(A):** Fundus photograph of an injected eye, 1 week post-transplantation. Note the numerous pigmented clusters formed by the transplanted hPSC-RPE cells. **(B):** Confocal micrograph showing the presence of rhodopsin-positive material (yellow arrows) within the cell membrane of carboxy-fluorescein diacetate succinimidyl ester-labeled hPSC-RPE cells, 1 week after subretinal injection. Scale bars = 10 μ m. Abbreviations: DAPI, 4',6-diamidino-2-phenylindole; ONL, outer nuclear layer; OS, outer segment; RPE, retinal pigment epithelium.

numbers of high-quality RPE cells. A single six-well plate containing 1.2×10^6 hPSCs, for instance, can produce up to 6×10^9 RPE cells at P2, which is up to 36 times more than the best protocols previously reported during the same time interval [22, 28, 30].

Since differentiation is achieved in monolayer, a standardized cell culture surface suitable for all stages of this process can be used to propagate hPSCs, obtain the initial RPE colonies, and further expand them. In addition, using simple culture media for RPE differentiation and culture, without the addition of serum, growth factors, or inhibitors, minimizes experimental variability while ensuring cost-efficient generation of differentiated cells. To our surprise, given the simplicity of our approach, we were able to obtain approximately 15% putative RPE cells after 50 days in differentiation medium, as assessed by RPE65 expression. RPE cell yield was not significantly different between our hiPSC and hESC lines, in accordance with previous studies [19, 52], whereas others reported lower efficiency with hiPSC lines [56, 57]. In the original report from Klimanskaya et al. [18], only 1% of EBs contained pigmented cells after 4–8 weeks. Using different cocktails of growth factors or small molecules, several subsequent studies reported RPE yields ranging from 25% to 33%, after several weeks, as assessed by MITF expression or the presence of pigmented cells [19, 21, 27, 58]. To date, the highest yield of RPE65+ cells observed after stepwise treatment with Nog-

gin, retinoic acid, and Sonic Hedgehog was approximately 40% [59]. Thus, although the RPE differentiation efficiency following our protocol is lower than that reported in recent studies, it is not considerably so.

Obtaining a pure and functional population devoid of contaminating cells is a key requirement for the use of hPSC-derived RPE cells in biomedical applications [31]. Concerning hESC-RPE cells, analysis by flow cytometry showed that the RPE cells obtained after serial passage had a purity of 98%–99%, depending on the RPE marker chosen, which is essentially the same as that obtained by manual picking. The high degree of cell purity obtained with hESC-RPE cells cultured on Matrigel or VN-PAS is comparable to that reported in a previous study, where hESC-RPE cells were purified by mechanical dissection and injected into human patients enrolled in a clinical trial [30].

In vivo applications, such as regenerative therapy, would greatly benefit from more defined and xeno-free conditions for hPSC-RPE cell production, since it could limit unwanted animal byproduct-induced immunogenicity or contamination from animal pathogens [60]. Most published protocols include feeder cells for hPSC propagation or differentiation and sometimes fetal bovine serum [32]. Recently, two studies described defined [57]

or xeno-free [61] conditions for RPE differentiation, yet in both cases, hPSCs were maintained on a layer of feeder cells.

With the use of VN-PAS, completely defined conditions were achieved for both hESC propagation and RPE generation. Because hiPSCs may be used to develop patient-specific therapy, we thought that it would be clinically relevant to reproduce with hiPSCs the results obtained with hESCs on VN-PAS. To our surprise, although analysis by flow cytometry showed the percentage of cells positive for marker expression to be >96% for both MITF and RPE65 when hiPSC-RPE cells were grown on Matrigel and for MITF when the cells were grown on VN-PAS, the percentage of RPE65+ cells cultured on VN-PAS was only 68%. Given the homogenous morphology of the hiPSC-RPE culture on VN-PAS and the absence of *PAX3* expression, contamination by melanocytes seems unlikely. Although we cannot formally exclude contamination by other MITF expressing cell types, an alternative hypothesis suggests that RPE cells from this specific hiPSC line (hiPSC IMR904) may not be maturing to the same level or at the same speed when grown on VN-PAS, compared with Matrigel. Further studies with an extended repertoire of hiPSC lines will be required to determine whether this result is a more general property of hiPSCs when VN-PAS is used for RPE generation.

In addition to marker expression, we also determined the fraction of functional cells within a given hPSC-RPE population. To this end we used a simple pH-Rhodo-labeled bioparticle phagocytosis assay described by Schwartz et al. [30]. With this approach, we observed similar percentages of functional hESC-RPE cells in their study and ours. By contrast, approximately 40% fewer hiPSC-RPE cells had phagocytosed bioparticles: importantly, hiPSC-RPE cells obtained by manual picking or serial passage performed equally, ruling out a possible negative effect from the latter procedure. These results are in contrast with a recent study of hiPSC-RPE cells from the same line that showed that 80%–90% of them had internalized fluorescent latex beads [53]. In another report, no difference was found between hESC-RPE and hiPSC-RPE cells for rod outer segment phagocytosis [22]. In both studies, different culture conditions were used for hiPSC-RPE culture. Although it is known that growth medium [62] and extracellular matrixes [63] can have an influence on RPE phagocytic activity, it remains unclear why in our hands this muted effect is only observed with hiPSC-RPE cells and not hESC-RPE cells.

Some variability was observed for *PAX6* expression following RPE purification by serial passage, with a higher level in hiPSC-RPE cells and a lower level in hESC-RPE cells, compared with RPE isolation by manual picking. Importantly, other key RPE transcription factors, such as *MITF* and *OTX2*, were left unchanged. Variable levels of *PAX6* expression have been observed in hPSC-RPE cells to date: it was clearly detected with hiPSC IMR90 and hESC H7 lines [18, 21–23, 27, 53], and in another study it was present with hESC lines but absent with hiPSC lines [52]. These different hPSC-RPE cell lines nevertheless expressed mature RPE markers and were functional [18, 21–23, 27, 52, 53]. Similarly, despite different *PAX6* expression levels, hESC-RPE and hiPSC-RPE cells obtained by serial passage secreted growth factors in a similar fashion. They also displayed the same degree of phagocytosis as their counterparts obtained by manual picking. Therefore, the variation in *PAX6* expression observed between hESC-RPE and hiPSC-RPE cells after serial passage may not be important enough to affect their identity as RPE cells.

Comparison studies have suggested that hiPSC-RPE cells display early senescence [22, 56] and differ more than hESC-RPE cells when compared with fetal RPE at the transcriptomic level [52]. However, others have demonstrated that hiPSC-RPE cells display many RPE functions [31]. Thus, it would be of interest to investigate with a large sample of hESC and hiPSC lines how RPE characteristics are affected when these cells are grown under a variety of conditions, so that differences inherent to ESCs and iPSCs may be uncovered. Such studies will be particularly relevant if hPSC-RPE cells were used as an in vitro model for drug screening or disease modeling.

CONCLUSION

In this report, we describe a new protocol for the generation of RPE from hPSCs, in which RPE cells are purified through two rounds of whole-dish single-cell dissociation. Together with clonal propagation of hPSCs, this differentiation process can be easily scaled up to allow the production of large amounts of highly purified and functional RPE cells. The monolayers of RPE cells demonstrated many characteristics of native RPE, including pigmentation and characteristic morphology, marker expression, polarized membrane and VEGF secretion, and phagocytic activity. We also show that the differentiation procedure can be achieved using totally defined conditions.

ACKNOWLEDGMENTS

We thank Dr. Alice Jouneau (INRA BDR) and Dr. Vinod Ranganathan (Johns Hopkins University) for help in reviewing the manuscript, Dr. Michael Young (Harvard Medical School) for fruitful discussions, Dr. Zara Melkounian (Corning Life Sciences) for useful advice regarding the use of VN-PAS, and Dr. Tomohiro Matsuda (Johns Hopkins University) for assistance with quantitative PCR experiments. This work was supported by a Foundation Fighting Blindness Wynn-Gund Translational Acceleration Program grant, an American Health Assistance Foundation Macular Degeneration Research grant, NIH Core Grant P30EY001765 to the Wilmer Eye Institute, unrestricted funds from Research to Prevent Blindness, Inc., and generous gifts from Mr. and Mrs. Robert and Clarice Smith, the Raab Family Foundation, and the Guerrieri Family Foundation. J.M. was supported by Post-Doctoral Fellowship Grant RFA-MD-11-3 from the Maryland Stem Cell Research Fund.

AUTHOR CONTRIBUTIONS

J.M.: conception and design, collection and assembly of data, data analysis and interpretation, manuscript writing, final approval of manuscript; K.W.: collection and assembly of data, data analysis and interpretation, manuscript reviewing; D.G.: collection and assembly of data; I.B.: collection of data; G.L.: data interpretation; D.J.Z.: conception and design, financial support, administrative support, data analysis and interpretation, manuscript writing, final approval of manuscript.

DISCLOSURE OF POTENTIAL CONFLICTS OF INTEREST

The VN-PAS Synthemax and Synthemax II SC and associated Corning products used in this study were provided without charge by Corning. J.M. received an honorarium and partial travel support from Corning to present this work at the 10th International Society for Stem Cell Research meeting.

REFERENCES

- 1 Gehrs KM, Anderson DH, Johnson LV et al. Age-related macular degeneration: Emerging pathogenetic and therapeutic concepts. *Ann Med* 2006;38:450–471.
- 2 Khandhadia S, Cherry J, Lotery AJ. Age-related macular degeneration. *Adv Exp Med Biol* 2012;724:15–36.
- 3 Strauss O. The retinal pigment epithelium in visual function. *Physiol Rev* 2005;85:845–881.
- 4 Curcio CA, Medeiros NE, Millican CL. Photoreceptor loss in age-related macular degeneration. *Invest Ophthalmol Vis Sci* 1996;37:1236–1249.
- 5 Schmier JK, Jones ML, Halpern MT. The burden of age-related macular degeneration. *Pharmacoeconomics* 2006;24:319–334.
- 6 Binder S, Stanzel BV, Krebs I et al. Transplantation of the RPE in AMD. *Prog Retin Eye Res* 2007;26:516–554.
- 7 da Cruz L, Chen FK, Ahmado A et al. RPE transplantation and its role in retinal disease. *Prog Retin Eye Res* 2007;26:598–635.
- 8 Caramoy A, Liakopoulos S, Menrath E et al. Autologous translocation of choroid and retinal pigment epithelium in geographic atrophy: Long-term functional and anatomical outcome. *Br J Ophthalmol* 2010;94:1040–1044.
- 9 Degenring RF, Cordes A, Schrage NF. Autologous translocation of the retinal pigment epithelium and choroid in the treatment of neovascular age-related macular degeneration. *Acta Ophthalmol* 2011;89:654–659.
- 10 Thomson JA, Itskovitz-Eldor J, Shapiro SS et al. Embryonic stem cell lines derived from human blastocysts. *Science* 1998;282:1145–1147.
- 11 Takahashi K, Tanabe K, Ohnuki M et al. Induction of pluripotent stem cells from adult human fibroblasts by defined factors. *Cell* 2007;131:861–872.
- 12 Yu J, Vodyanik MA, Smuga-Otto K et al. Induced pluripotent stem cell lines derived from human somatic cells. *Science* 2007;318:1917–1920.
- 13 Maruotti J, Jouneau A, Renard JP. Faithful reprogramming to pluripotency in mammals, what does nuclear transfer teach us? *Int J Dev Biol* 2010;54:1609–1621.
- 14 Hu Q, Friedrich AM, Johnson LV et al. Memory in induced pluripotent stem cells: Reprogrammed human retinal pigmented epithelial cells show tendency for spontaneous redifferentiation. *STEM CELLS* 2010;28:1981–1991.
- 15 Tobin SC, Kim K. Generating pluripotent stem cells: Differential epigenetic changes during cellular reprogramming. *FEBS Lett* 2012;586:2874–2881.
- 16 Kawasaki H, Suemori H, Mizuseki K et al. Generation of dopaminergic neurons and pigmented epithelia from primate ES cells by stromal cell-derived inducing activity. *Proc Natl Acad Sci USA* 2002;99:1580–1585.
- 17 Haruta M, Sasai Y, Kawasaki H et al. In vitro and in vivo characterization of pigment epithelial cells differentiated from primate embryonic stem cells. *Invest Ophthalmol Vis Sci* 2004;45:1020–1025.
- 18 Klimanskaya I, Hipp J, Rezai KA et al. Derivation and comparative assessment of retinal pigment epithelium from human embryonic stem cells using transcriptomics. *Cloning Stem Cells* 2004;6:217–245.
- 19 Osakada F, Jin ZB, Hiram Y et al. In vitro differentiation of retinal cells from human pluripotent stem cells by small-molecule induction. *J Cell Sci* 2009;122:3169–3179.
- 20 Hiram Y, Osakada F, Takahashi K et al. Generation of retinal cells from mouse and human induced pluripotent stem cells. *Neurosci Lett* 2009;458:126–131.
- 21 Meyer JS, Shearer RL, Capowski EE et al. Modeling early retinal development with human embryonic and induced pluripotent stem cells. *Proc Natl Acad Sci USA* 2009;106:16698–16703.
- 22 Buchholz DE, Hikita ST, Rowland TJ et al. Derivation of functional retinal pigmented epithelium from induced pluripotent stem cells. *STEM CELLS* 2009;27:2427–2434.
- 23 Carr AJ, Vugler AA, Hikita ST et al. Protective effects of human iPSC-derived retinal pigment epithelium cell transplantation in the retinal dystrophic rat. *PLoS One* 2009;4:e8152.
- 24 Lee E, MacLaren RE. Sources of retinal pigment epithelium (RPE) for replacement therapy. *Br J Ophthalmol* 2011;95:445–449.
- 25 Juuti-Uusitalo K, Vaajasaari H, Ryhanen T et al. Efflux protein expression in human stem cell-derived retinal pigment epithelial cells. *PLoS One* 2012;7:e30089.
- 26 Vugler A, Carr AJ, Lawrence J et al. Elucidating the phenomenon of HESC-derived RPE: Anatomy of cell genesis, expansion and retinal transplantation. *Exp Neurol* 2008;214:347–361.
- 27 Idelson M, Alper R, Obolensky A et al. Directed differentiation of human embryonic stem cells into functional retinal pigment epithelium cells. *Cell Stem Cell* 2009;5:396–408.
- 28 Lu B, Malcuit C, Wang S et al. Long-term safety and function of RPE from human embryonic stem cells in preclinical models of macular degeneration. *STEM CELLS* 2009;27:2126–2135.
- 29 Lund RD, Wang S, Klimanskaya I et al. Human embryonic stem cell-derived cells rescue visual function in dystrophic RCS rats. *Cloning Stem Cells* 2006;8:189–199.
- 30 Schwartz SD, Hubschman JP, Heilwell G et al. Embryonic stem cell trials for macular degeneration: A preliminary report. *Lancet* 2012;379:713–720.
- 31 Bharti K, Miller SS, Arnheiter H. The new paradigm: Retinal pigment epithelium cells generated from embryonic or induced pluripotent stem cells. *Pigment Cell Melanoma Res* 2011;24:21–34.
- 32 Rowland TJ, Buchholz DE, Clegg DO. Pluripotent human stem cells for the treatment of retinal disease. *J Cell Physiol* 2012;227:457–466.
- 33 Walker A, Su H, Conti MA et al. Non-muscle myosin II regulates survival threshold of pluripotent stem cells. *Nat Commun* 2010;1:71.
- 34 Chen G, Hou Z, Gulbranson DR et al. Actin-myosin contractility is responsible for the reduced viability of dissociated human embryonic stem cells. *Cell Stem Cell* 2010;7:240–248.
- 35 Melkounian Z, Weber JL, Weber DM et al. Synthetic peptide-acrylate surfaces for long-term self-renewal and cardiomyocyte differentiation of human embryonic stem cells. *Nat Biotechnol* 2010;28:606–610.
- 36 Gamm DM, Melvan JN, Shearer RL et al. A novel serum-free method for culturing human prenatal retinal pigment epithelial cells. *Invest Ophthalmol Vis Sci* 2008;49:788–799.
- 37 Klimanskaya I. Retinal pigment epithelium. *Methods Enzymol* 2006;418:169–194.
- 38 Tolosa JM, Schjenken JE, Civiti TD et al. Column-based method to simultaneously extract DNA, RNA, and proteins from the same sample. *BioTechniques* 2007;43:799–804.
- 39 Ungrin M, O'Connor M, Eaves C et al. Phenotypic analysis of human embryonic stem cells. *Curr Protoc Stem Cell Biol* 2007;Chapter 1:Unit 1B.3.
- 40 Synnregren J, Giesler TL, Adak S et al. Differentiating human embryonic stem cells express a unique housekeeping gene signature. *STEM CELLS* 2007;25:473–480.
- 41 Bharti K, Nguyen MT, Skuntz S et al. The other pigment cell: Specification and development of the pigmented epithelium of the vertebrate eye. *Pigment Cell Res* 2006;19:380–394.
- 42 Sperger JM, Chen X, Draper JS et al. Gene expression patterns in human embryonic stem cells and human pluripotent germ cell tumors. *Proc Natl Acad Sci USA* 2003;100:13350–13355.
- 43 Maminishkis A, Chen S, Jalickee S et al. Confluent monolayers of cultured human fetal retinal pigment epithelium exhibit morphology and physiology of native tissue. *Invest Ophthalmol Vis Sci* 2006;47:3612–3624.
- 44 Marmorstein AD, Marmorstein LY, Rayborn M et al. Bestrophin, the product of the Best vitelliform macular dystrophy gene (VMD2), localizes to the basolateral plasma membrane of the retinal pigment epithelium. *Proc Natl Acad Sci USA* 2000;97:12758–12763.
- 45 Rizzolo LJ. Development and role of tight junctions in the retinal pigment epithelium. *Int Rev Cytol* 2007;258:195–234.
- 46 Määttä M, Tervahartiala T, Kaarniranta K et al. Immunolocalization of EMMPRIN (CD147) in the human eye and detection of soluble form of EMMPRIN in ocular fluids. *Curr Eye Res* 2006;31:917–924.
- 47 Steele FR, Chader GJ, Johnson LV et al. Pigment epithelium-derived factor: Neurotrophic activity and identification as a member of the serine protease inhibitor gene family. *Proc Natl Acad Sci USA* 1993;90:1526–1530.
- 48 Vollrath D, Feng W, Duncan JL et al. Correction of the retinal dystrophy phenotype of the RCS rat by viral gene transfer of Mertk. *Proc Natl Acad Sci USA* 2001;98:12584–12589.
- 49 Gong J, Sagiv O, Cai H et al. Effects of extracellular matrix and neighboring cells on induction of human embryonic stem cells into retinal or retinal pigment epithelial progenitors. *Exp Eye Res* 2008;86:957–965.
- 50 Martínez-Morales JR, Rodrigo I, Bovolenta P. Eye development: A view from the retina pigmented epithelium. *Bioessays* 2004;26:766–777.
- 51 Masuda T, Esumi N. SOX9, through interaction with microphthalmia-associated transcription factor (MITF) and OTX2, regulates BEST1 expression in the retinal pigment epithelium. *J Biol Chem* 2010;285:26933–26944.
- 52 Liao JL, Yu J, Huang K et al. Molecular signature of primary retinal pigment epithelium and stem-cell derived RPE cells. *Hum Mol Genet* 2010;19:4229–4238.

53 Kokkinaki M, Sahibzada N, Golestaneh N. Human iPS-derived retinal pigment epithelium (RPE) cells exhibit ion transport, membrane potential, polarized VEGF secretion and gene expression pattern similar to native RPE. *STEM CELLS* 2011;29:825–835.

54 Widlund HR, Fisher DE. Microphthalmia-associated transcription factor: A critical regulator of pigment cell development and survival. *Oncogene* 2003;22:3035–3041.

55 Amann PM, Luo C, Owen RW et al. Vitamin A metabolism in benign and malignant melanocytic skin cells: Importance of lecithin/retinol acyltransferase and RPE65. *J Cell Physiol* 2012;227:718–728.

56 Feng Q, Lu SJ, Klimanskaya I et al. Hemangioblastic derivatives from human induced pluripotent stem cells exhibit limited expan-

sion and early senescence. *STEM CELLS* 2010;28:704–712.

57 Rowland TJ, Blaschke AJ, Buchholz DE et al. Differentiation of human pluripotent stem cells to retinal pigmented epithelium in defined conditions using purified extracellular matrix proteins. *J Tissue Eng Regen Med* 2012 [Epub ahead of print].

58 Osakada F, Ikeda H, Mandai M et al. Toward the generation of rod and cone photoreceptors from mouse, monkey and human embryonic stem cells. *Nat Biotechnol* 2008;26:215–224.

59 Zahabi A, Shahbazi E, Ahmadi H et al. A new efficient protocol for directed differentiation of retinal pigmented epithelial cells from normal and retinal disease induced pluripotent stem cells. *Stem Cells Dev* 2012;21:2262–2272.

60 Mallon BS, Park KY, Chen KG et al. Toward xeno-free culture of human embryonic stem cells. *Int J Biochem Cell Biol* 2006;38:1063–1075.

61 Vaajasaari H, Ilmarinen T, Juuti-Uusitalo K et al. Toward the defined and xeno-free differentiation of functional human pluripotent stem cell-derived retinal pigment epithelial cells. *Mol Vis* 2011;17:558–575.

62 Karl MO, Valtink M, Bednarz J et al. Cell culture conditions affect RPE phagocytic function. *Graefes Arch Clin Exp Ophthalmol* 2007;245:981–991.

63 Miceli MV, Newsome DA. Effects of extracellular matrix and Bruch's membrane on retinal outer segment phagocytosis by cultured human retinal pigment epithelium. *Curr Eye Res* 1996;15:17–26.



See www.StemCellsTM.com for supporting information available online.